Applied Chemical Engineering (2022) Volume 5 Issue 2
doi:10.24294/ace.v5i2.1640

ORIGINAL RESEARCH ARTICLE

Nickel particle/graphene composite as a new matrix-assisted laser desorption ionization mass spectrometry matrix and adsorbent for high performance mass spectrometry analysis of biological small molecules

Huifang Zhao[1,2], Huayu Zhao[2], Siwen Yi[1], Ruiping Zhang[2*]

[1] *School of Basic Medical Sciences, Shanxi Medical University, Taiyuan 030001, Shanxi Province, China.*

[2] *Shanxi Bethune Hospital, the Third Hospital of Shanxi Medical University, Taiyuan 030032, Shanxi Province, China.*

E-mail: zrp_7142@sxmu.edu.cn

ABSTRACT

Using the synthesized nickel particle/graphene (Ni/Gr) composite as a new matrix and adsorbent, a matrix-assisted laser desorption ionization time of flight mass spectrometry (MALDI-TOF MS) platform was constructed for the efficient analysis of various drugs, amino acids and other small biological molecules. Compared with the traditional matrix of 2, 5-dihydroxyphenyl acid (DHB) and a series of comparison materials (Gr, Ni-1/gr and Ni-5/gr), Ni-2/gr as MALDI matrix has the advantages of low background noise, high ionic strength, high signal-to-noise ratio and wide linear range (0.01 ~ 50 μmol/L, 0.2 ~ 50 μmol/L and 0.05 ~ 60 μmol/L) when analyzing the molecules of resveratrol, 6-gingerol and rutin in the positive ion mode. The detection limits (LODs) of resveratrol, 6-gingerol and rutin were respectively 0.0038, 0.09 and 0.02 μmol/L. Ni-2/gr complex has the characteristics of high specific surface area, rich mesoporous structure, a large number of sp^2 structures, strong UV absorption and high saturation magnetization value (MS). It can be used as an adsorbent to magnetically enrich phenylalanine, tryptophan and tyrosine, and can also be used to magnetically enrich low concentration tryptophan in mouse serum samples.

Keywords: Nickel Particles/Graphene; Matrix-Assisted Laser Desorption Time-of-Flight Mass Spectrometry; Drug Molecules; Amino Acid; Adsorbent

ARTICLE INFO

Received: 17 May 2022
Accepted: 18 July 2022
Available online: 6 August 2022

1. Introduction

Matrix-assisted laser desorption time-of-flight mass spectrometry (MALDI-TOF MS) is a new soft ionization biological mass spectrometry technology developed in the late 1980s[1,2], which has the advantages of simple sample pretreatment, fast analysis speed, good salt tolerance and high sensitivity. It has been widely used in the analysis of biological macromolecules such as proteins, peptides, nucleic acids[3–5]. However, commonly used α-cyano-4-hydroxybenzoic acid (CHCA), 2, 5-dihydroxybenzoic acid (DHB), sinapic acid (SA) and other organic acid substrates have a large number of matrix background interference peaks in the range of m/z < 1,000, which seriously limits the application of MALDI-TOF MS in drug analysis and endogenous biological small molecule detection.

In recent years, researchers have used various types of nanomaterials such as porous silicon[6,7], metal particles[8–10], metal oxides[11,12], metal organic frameworks[13,14] and carbon-based materials[15–19] to replace the traditional organic acid matrix for the analysis compounds with low molecular weight. Among them, graphene-based

carbon materials show good performance in the analysis of small biological molecules such as drugs, amino acids and sugars by MALDI-TOF MS due to their large specific surface area, good optical absorption and high electron transfer ability[15,20,21]. In order to further improve the ionization efficiency of the analyte to be tested, it has been reported that the introduction of transition metals (iron, cobalt and nickel) into carbon-based complexes can enhance the adsorption capacity[22–24] and promote the desorption and ionization of small molecules. Li *et al*.[25] prepared cobalt particle/porous carbon complex as a new MALDI matrix with high adsorption performance for the analysis of small molecular metabolites in rat liver microdialysis solution. However, up to now, it has not been reported that nickel particles/carbon-based complexes are used as adsorbents for MALDI-TOF MS analysis of small biomolecules.

In this study, a series of composite materials with different contents of nickel particles loaded on graphene (Ni/Gr) were prepared, which were used as new MALDI matrix and adsorbent, respectively for the efficient analysis of different types of biological small molecules such as drugs and amino acids by MS. The results show that compared with traditional DHB matrix and comparison materials (Gr, Ni-1/Gr and Ni-5/Gr), Ni-2/Gr matrix has the advantages of low background noise, high ionic signal, high signal-to-noise ratio and high sensitivity when analyzing resveratrol, 6-gingerol and rutin, and has strong adsorption and enrichment ability for low concentrations of phenylalanine, tryptophan and tyrosine, successfully realizing the enrichment of tryptophan molecules in mouse serum.

2. Experimental part

2.1 Instruments and reagents

JEOL JEM-2100F transmission electron microscope (Hitachi, Ltd., Japan); D8 ADVANCE X-ray diffractometer, Ultraflextreme matrix-assisted laser desorption time-of-flight mass spectrometer (Bruker, Germany); DXR 2xi Raman spectrometer (Thermo Fisher Scientific, USA); ASAP 2020 BET specific surface area analyzer (Micromeritics Instrument Corporation, USA); Axis Ultra DLD X-ray photoelectron spectrometer (Kratos Analytical Limited, UK); UV270 ultraviolet-visible absorption spectrometer (Shimadzu Corporation, Japan); MPMS vibrating sample magnetometer (Quantum Corporation, USA); EXPLORER^{TM} analytical balance (Ohaus Corporation, USA.); Model 85-2 magnetic stirrer (Hangzhou Ruijia Precision Scientific Instrument Co., Ltd.); LGJ-10 vacuum freeze dryer (Beijing Songyuan Huaxing Technology Development Co., Ltd.); OTF-1200X tubular furnace (Hefei Kejing Co., Ltd.); Milli-Q ultra pure water meter (Merck & Co., Inc., USA).

Graphite powder (purity 99.95%, Qingdao China Resources Graphite Co., Ltd.); Nickel acetate tetrahydrate (Ni $(AC)_2{\cdot}4H_2O$, AR), resveratrol (99%), 6-gingerol (98%), rutin (98%), phenylalanine (BR), tryptophan (BR) and tyrosine (BR) (Sinopharm Chemical Reagent Co., Ltd.); polyvinyl alcohol (PVA, molecular weight 30,000 ~ 70,000) and 2, 5-dihydroxybenzoic acid (DHB, 98%) (Sigma-Aldrich Corporation, USA).

2.2 Preparation of Ni/Gr composites

GR was synthesized by electrochemical method[26,27]. Dissolve 2.0 mmol/L Ni $(Ac)_2{\cdot}4H_2O$ in 10 ml PVA (10 mg/mL) solution to obtain a transparent green solution. Slowly add the above solution to the pre-synthesized GR solution (2 mg/mL), stir overnight at room temperature, and freeze dry. Then, in H_2-AR (1:9, *V/V*) atmosphere, the composite of nickel particle-supported graphene (Ni-2/Gr) was obtained by keeping it at 600 °C for 2 hours and cooling it to room temperature. Using the same method, Ni-1/Gr (1.0 mmol/L $Ni(Ac)_2{\cdot}4H_2O$) and Ni-5/Gr (5.0 mmol/l $Ni(Ac)_2{\cdot}4H_2O$) composites were synthesized.

2.3 Preparation of mouse serum samples

The whole blood samples of mice were from three male C57BL/6 mice aged 5 months, which were provided by the animal center of Shanxi Medical University. All animal experiments met the requirements of the animal ethics committee of Shanxi Medical University. Take the above 0.1 mL whole blood sample and add it to the methanol so-

lution to precipitate the protein to obtain the serum solution. After centrifugation at 1,750 r/min for 8 minutes, collect the supernatant and store it at −80 °C for mass spectrometry analysis.

2.4 Preparation of standard sample and matrix

Resveratrol and 6-gingerol are dissolved in 50% (*V/V*) ethanol solution to prepare 1 mmol/L reserve solution, rutin is dissolved in 50% (*V/V*) acetonitrile solution to prepare 1 mmol/L reserve solution; phenylalanine and tryptophan are dissolved in water to prepare a 1 mmol/L reserve solution, and tyrosine is dissolved in 50% (*V/V*) formic acid solution to prepare a 1 mmol/L reserve solution. Analytes of different concentrations are obtained by diluting the reserve solution. DHB (20 mg/mL) is dissolved in methanol water (7:3, *V/V*) solution containing 0.1% trifluoroacetic acid. Ni-1/Gr (1 mg/mL), Ni-2/Gr (1 mg/mL) and Ni-5/Gr (1 mg/mL) complexes were dispersed in 50% (*V/V*) ethanol solution as a new MALDI carbon matrix.

2.5 MALDI-TOF MS analysis

The above matrix solution (1 μL) was dropped onto the MALDI stainless steel target plate, and after natural drying, different types and concentrations of analytes were added onto the above matrix-containing target plate, and then analyzed with MALDI-TOF MS after dried thoroughly at room temperature. The calibration of MALDI MS uses DHB matrix, and MS measurement adopts positive ion reflection mode. In the range of *m/z* 100 ~ 1,000, the repetition rate is 1,000, and the laser intensity is 50%. The spectra were collected continuously, and the data were processed by Flex Analysis (Bruker) software.

2.6 Ni-2/Gr as adsorbent for MALDI-TOF MS analysis

10 mg Ni-2/Gr was dissolved in 1 mL of 50% (*V/V*) ethanol solution, sonicated for 0.5 h, 50 μL of the above solution was quickly added dropwise to 500 μL of 50 μmol/L amino acid solution. After stirring the mixed solution for 30 minutes, magnetic separation is carried out under the action of an external magnet, and 1 μL of the enriched solution is dropped on the MALDI target plate and dried naturally for MALDI MS snslysis of amino acid molecules.

3. Results and discussion

3.1 Characterization of Ni/Gr composites

Ni/Gr composites were prepared by high temperature thermal reduction (**Figure 1**). According to the transmission electron microscope (TEM) image (**Figure 1A**), GR is a lamellar structure with some folds on the surface; When Ni/Gr composites with different sizes were prepared by high temperature thermal reduction, nickel particles were uniformly loaded on the surface of the lamellar GR, and the size of nickel particles increased with the increase of $Ni(Ac)_2{\cdot}4H_2O$ concentration (**Figures 1B** ~ **1D**). It can be seen from the inner illustrations in **Figures 1b** to **1D** that the average particle sizes of nickel particles in Ni-1/Gr, Ni-2/Gr and Ni-5/Gr composites are 16.95 nm, 27.22 nm and 39.03 nm, respectively.

The crystal form of Ni/Gr composite was characterized by X-ray diffraction (XRD). As shown in **Figure 2A**, graphite carbon with (002) crystal plane appears in Ni-1/Gr, Ni-2/Gr and Ni-5/Gr at 25.6° (PDF No. 41–1,487). At the same time, the (111), (200) and (220) crystal planes of Ni nanoparticles (PDF No. 87–0712) correspond to 44.50°, 51.85° and 76.38°, respectively[28]. Moreover, with the increase of nickel particle size, the strength of the corresponding Ni crystal plane increases, and the strength of the corresponding carbon (002) crystal plane in the composite decreases. The graphitization degree of Ni/Gr composite was characterized by Raman spectroscopy (**Figure 2B**). All Ni/Gr composites have D peak (~ 1,345 cm^{-1}) and G peak (~ 1,590 cm^{-1}), corresponding to sp^3 defective carbon and sp^2 graphite carbon, respectively[29]. The I_D/I_G corresponding to Ni-1/Gr, Ni-2/Gr and Ni-5/Gr are 1.044, 0.9329 and 0.9536, respectively. Ni-2/Gr composite has the highest graphitization degree, and its use as MALDI-TOF MS matrix will help to enhance the ionization efficiency of small molecules. As shown in **Figure 2C**, the adsorption desorption curve of N_2 shows that

the BET specific surface areas corresponding to Ni-1/Gr, Ni-2/Gr and Ni-5/Gr are 138.32, 91.14 and 46.59 m^2/g, respectively. Meanwhile, all Ni/Gr materials mainly exist in the form of mesopores (**Figure 2D**). The large specific surface area and abundant mesoporous structure are conducive to the adsorption of more small molecules in the MALDI-TOF MS analysis process[25], which is beneficial to the desorption and ionization of the target.

The surface chemical composition and electronic structure of Ni/Gr composites were characterized by X-ray photoelectron spectroscopy (XPS). It can be seen from **Figure 3A** that the full spectrum peaks of Ni-1/Gr, Ni-2/Gr and Ni-5/Gr complexes are composed of carbon (C), oxygen (O) and nickel (Ni). Taking Ni-2/Gr complex as an example, high-resolution peak splitting analysis of C and Ni elements (**Figure 3B**), C 1s in Ni-2/Gr corresponds to sp^2 C = C, sp^3 C-C, C-O and C(O)O peaks at 284.6, 285.5, 286.6 and 289.2 eV, respectively[30]. **Figure 3C** shows that Ni 2p in Ni-2/Gr is composed of Ni $2p_{3/2}$, Ni $2p_{1/2}$ and satellite peaks. The spectral peaks at 852.8 and 855.7 eV belong to Ni^0 and Ni^{2+} of Ni-2/Gr corresponding to Ni $2p_{3/2}$[28], indicating that Ni elements mainly exist in the form of metal.

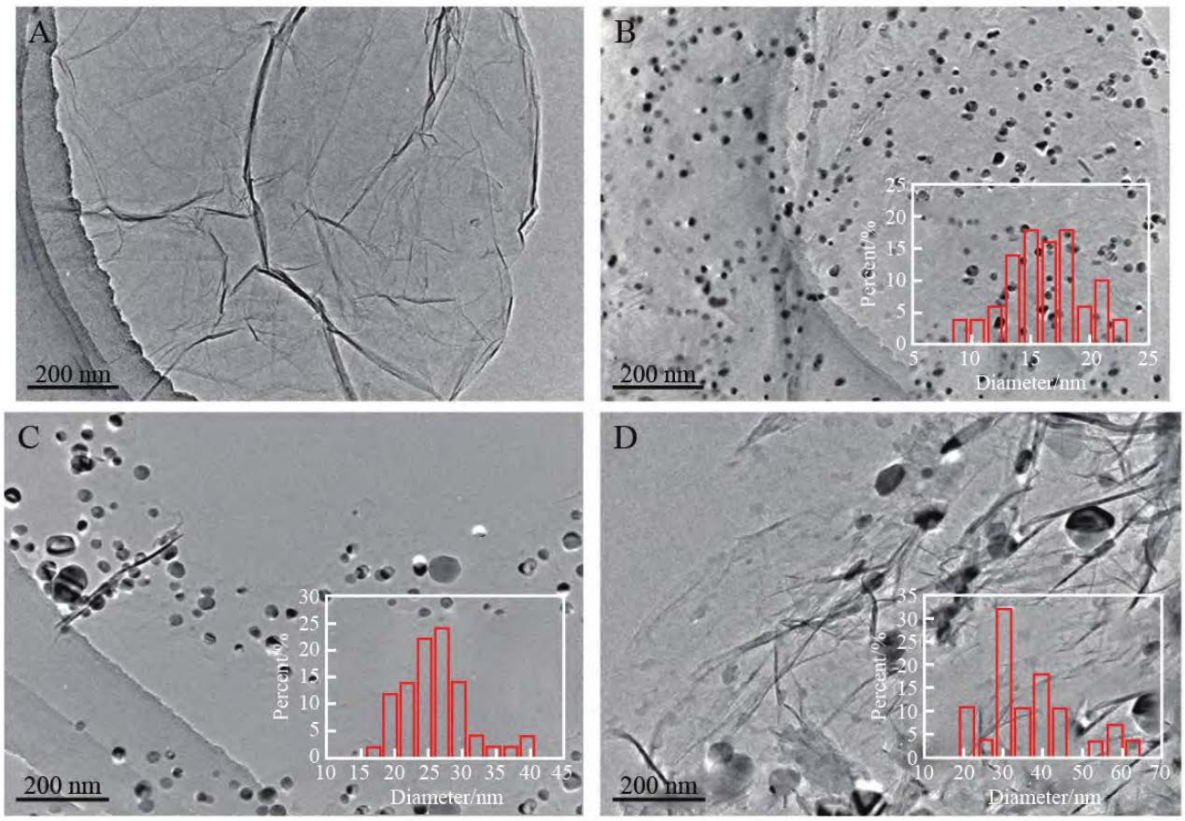

Figure 1. Transmission electron microscopy (TEM) images of (**A**) graphene (Gr), (**B**) Ni-1/Gr, (**C**) Ni-2/Gr and (**D**) Ni-5/Gr. Inset of (B-D): size distribution of Ni nanoparticles with different contents.

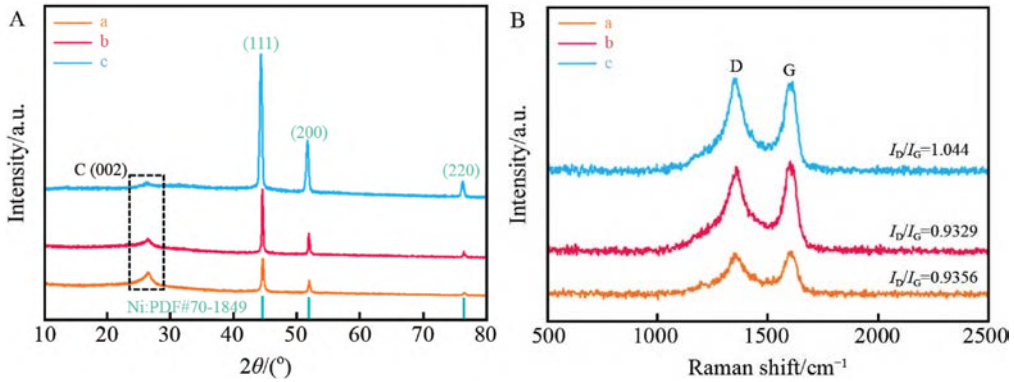

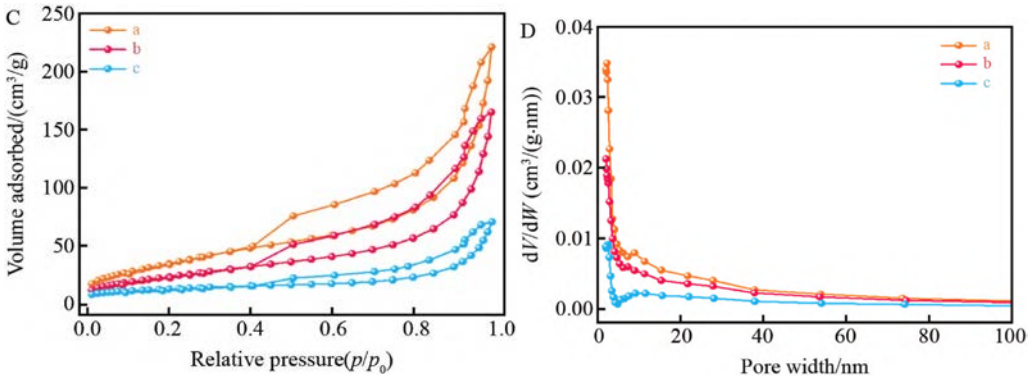

Figure 2. (**A**) X-ray diffraction (XRD) patterns, (**B**) Raman spectra, (**C**) N_2 adsorption-desorption isotherms and (**D**) pore size-distribution curves of (a) Ni-1/Gr, (b) Ni-2/Gr and (c) Ni-5/Gr.

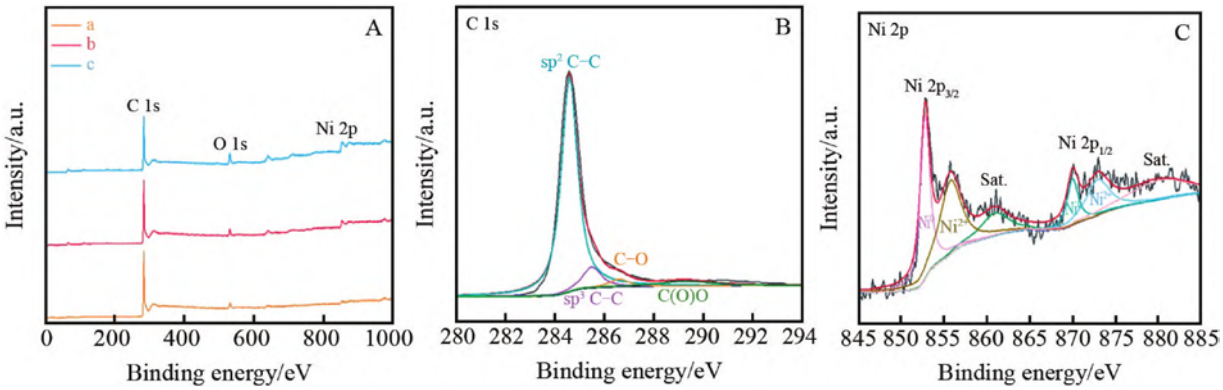

Figure 3. (**A**) The full X-ray photoelectron spectra (XPS) of (a) Ni-1/Gr, (b) Ni-2/Gr and (c) Ni-5/Gr; High-resolution XPS spectra of (**B**) C 1s and (**C**) Ni 2p of Ni-2/Gr.

3.2 Analysis of drug molecules based on MALDI-TOF MS

Using traditional organic acids DHB, GR, Ni-1/Gr, Ni-2/Gr and Ni-5/Gr as MALDI matrix, the ionization behavior of resveratrol was analyzed in positive ion mode. As shown in **Figure 4A**, when DHB is used as the matrix (curve a), the low intensity $[M + H]^+$ peak of resveratrol is only observed at *m/z* 229.025, and has a low signal-to-noise ratio (*S/N*); With GR as the matrix (curve b), the low ionic strength $[M + Na]^+$ and $[M + K]^+$ peaks of resveratrol can be observed at *m/z* 251.013 and 267.064, and there is also a small amount of background noise. When using Ni-1/Gr (curve c) and Ni-5/Gr (curve e) matrixs, the $[M + H]^+$ peak of resveratrol appears at *m/z* 229.025, and its corresponding *S/N* value is higher than that of DHB matrix. At the same time, the $[M + Na]^+$ peak of resveratrol is also observed at *m/z* 251.013, and its corresponding *S/N* value is higher than that of GR matrix. Although Ni-1/Gr and Ni-5/Gr as MALDI matrix analysis of resveratrol, the corresponding adduct peak ion strength of positive ion, *S/N* and ion species are better than traditional DHB and GR, when Ni-2/Gr is used as MALDI matrix (curve d), not only the $[M + H]^+$ and $[M + Na]^+$ peaks of resveratrol, but also the corresponding $[M + K]^+$, $[M + 2Na\text{-}H]^+$ and $[M + 3Na\text{-}2H]^+$ peaks can be observed, and the intensity and *S/N* ratio of various ion peaks are higher than Ni-1/Gr and Ni-5/Gr. The molecular formula of resveratrol, the analyte to be tested, is shown in **Figure 4B**, and the strength of the cationic adduct peak of resveratrol under different matrices is shown in **Figure 4C**. The results show that when using Ni-2/Gr complex as MALDI matrix to analyze resveratrol mass spectrometry, it has low background noise, high ionization intensity and high *S/N* value, showing a good analytical effect.

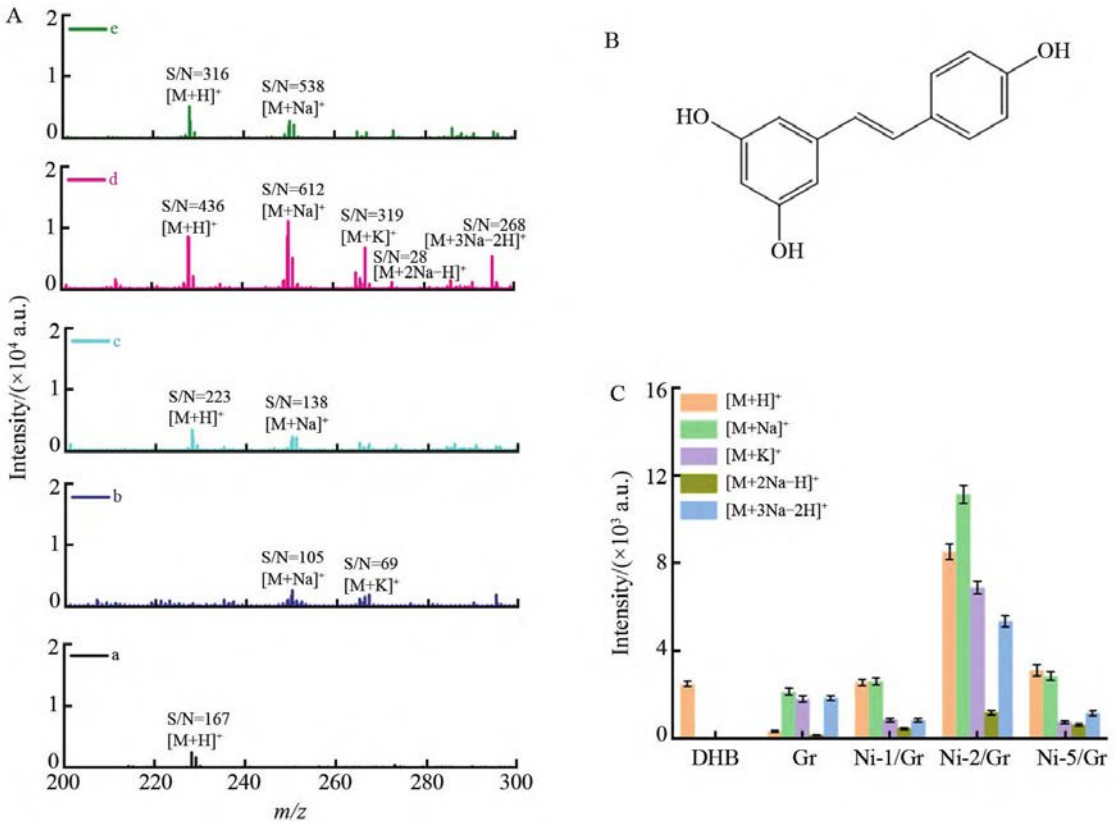

Figure 4. (**A**) Comparison of performances of matrix-assisted laser desorption/ionization time-of-flight mass spectroscopy (MALDI-TOF MS) analysis of resveratrol (20 μmol/L) using various matrices including (a) 2, 5-dihydroxybenzoic acid (DHB), (b) Gr, (c) Ni-1/Gr, (d) Ni-2/Gr and (e) Ni-5/Gr in positive-ion mode; (**B**) structural formula of resveratrol; (**C**) MS intensities of all cationic additive peaks of resveratrol with various matrices (n = 5).

In the positive ion mode, the mass ionization properties of 6-gingerol and rutin were investigated, respectively. As shown in **Figure 5A**, when DHB matrix is used (curve a), in addition to the low-intensity $[M + Na]^+$ and $[M + K]^+$ peaks of 6-gingerol observed at *m/z* 317.069 and 333.018, there is also a strong background ion interference peak, which seriously affects its *S/N* value. When Gr (curve b), Ni-1/Gr (curve C), Ni-2/Gr (curve d) and Ni-5/Gr (curve e) matrices are used, only the $[M + Na]^+$ and $[M + K]^+$ peaks of 6-gingerol are observed. When Ni-2/Gr is used as MALDI matrix, the intensity of the $[M + Na]^+$ and $[M + K]^+$ peaks of 6-gingerol is the highest, and the corresponding *S/N* value is also the highest. Similarly, when DHB (curve a), Gr (curve b), Ni-1/Gr (curve c), Ni-2/Gr (curve d) and Ni-5/Gr (curve e) matrix were used, the $[M + Na]^+$ and $[M + K]^+$ peaks of rutin at *m/z* 633.042 and 649.037 could be detected (**Figure 5B**). However, considering the factors such as ionic strength and *S/N* ratio, Ni-2/Gr complex as MALDI matrix is more suitable for highly sensitive analysis of rutin. In conclusion, using Ni-2/Gr as a new MALDI matrix to analyze resveratrol, 6-gingerol and rutin has excellent ionization performance.

Before using Ni-2/Gr matrix to efficiently and quantitatively detect resveratrol, 6-gingerol and rutin, reproducibility is an important index to be investigated. For three target analytes (20 μmol/L) to analyze the relative standard deviation (RSD) of peak intensity at 8 different positions (shot to shot) in the same sample point and 10 different target points (spot to spot) of a sample. It can be seen from **Table 1** that the RSD value is in the range of 4.4% to 10.3%, indicating that the Ni-2/Gr matrix assisted MALDI mass spectrometry method has good reproducibility.

Table 1. Shot-to-shot and spot-to-spot repeatability of ion intensities obtained by Ni-2/Gr assisted MALDI MS

Target	**Shot-to-shot (RSD, %, n = 8)**	**Spot-to-spot (RSD, %, n = 10)**
Resveratrol	6.72	10.32
6-6-Giiigerol	4.38	8.17
Rutin	6.01	9.29

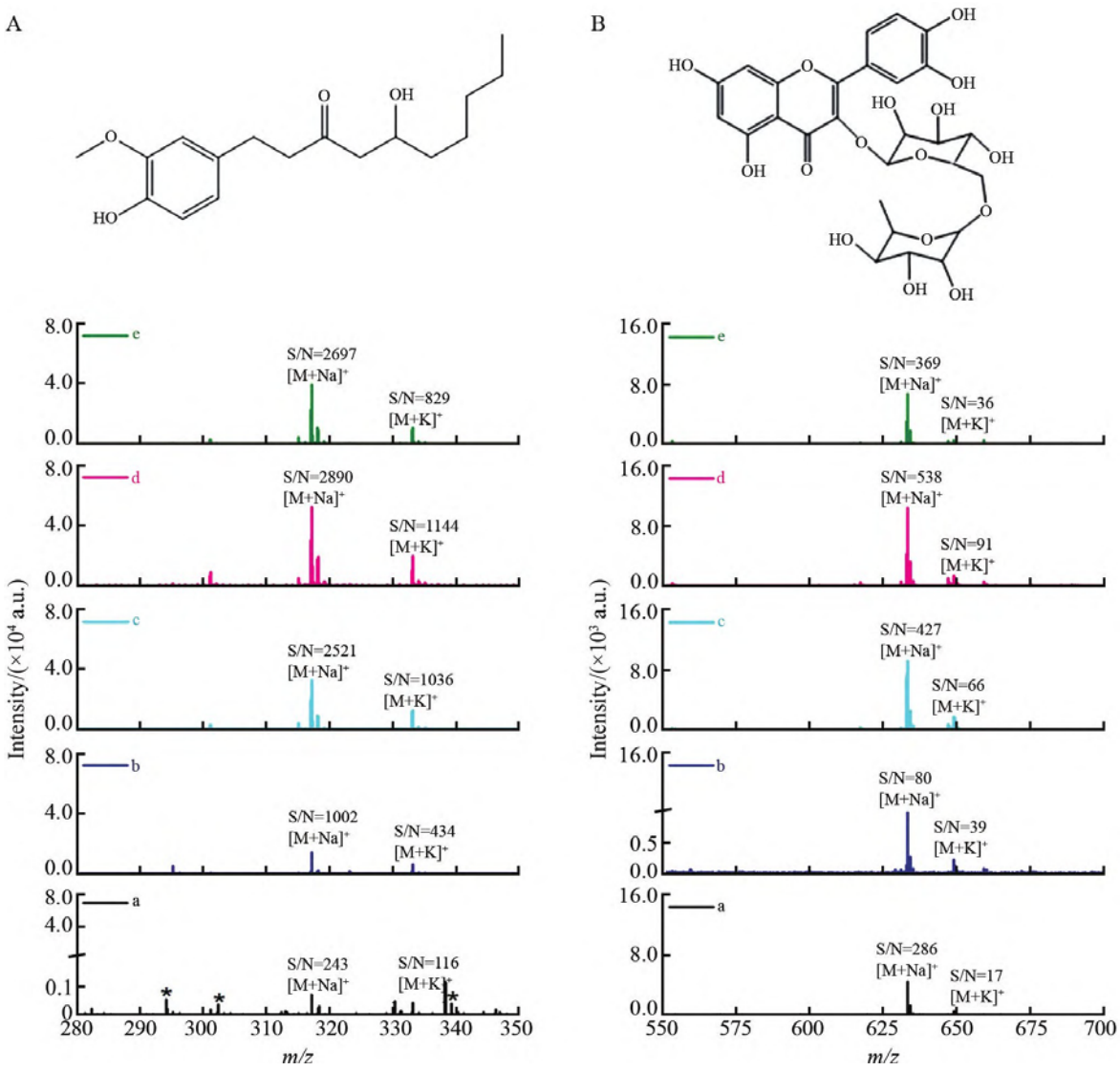

Figure 5. MALDI MS performance of positive-ion of (**A**) 6-gingerol and (**B**) rutin with various matrices: (a) DHB; (b) Gr; (c) Ni-1/Gr; (d) Ni-2/Gr; (e) Ni-5/Gr.
Note: The concentrations of 6-gingerol and rutin are 50 μmol/L, respectively. *represents the background noise from matrix.

1.0 μL synthesized Ni-2/Gr matrix and 1.0 μL samples of different concentrations of resveratrol, 6-gingerol and rutin were dropped on the MALDI target plate to determine the ionization intensity of the corresponding analyte. As shown in **Figure 6**, the concentrations of resveratrol (**Figure 6A**) and rutin (**Figure 6C**) have a linear relationship with their $[M + Na]^+$ peak intensity, and the concentration of 6-gingerol has a linear relationship with the *S/N* ratio corresponding to the measured $[M + Na]^+$ peak (**Figure 6B**). The ionic strength corresponding to each concentration was collected repeatedly for 3 times, and resveratrol showed a good linear relationship with its corresponding $[M + Na]^+$ peak intensity in the concentration range of 0.01 ~ 50 μmol/L (**Figure 6A**), and 6-gingerol was in 0.01–50 μmol/L concentration range. The *S/N* ratio corresponding to its $[M + Na]^+$ peak has a good linear relationship in the concentration range of 2 ~ 50 μmol/L (**Figure 6B**), and the corresponding S/N ratio of rutin in the concentration range of 0.05 ~ 60 μmol/L The $[M + Na]^+$ peak intensity has a good linear relationship (**Figure 6C**). The detection limits (LODs, *S/N* = 3) of resveratrol, 6-gingerol and rutin were 0.0038, 0.09 and 0.02 μmol/L, respectively. The performance indexes of resveratrol, 6-gingerol and rutin are shown in **Table 2** by using Ni-2/Gr matrix for highly sensitive analysis. The LOD value of resveratrol analyzed by MALDI MS method is far lower than the electrochemical method[31,32] and

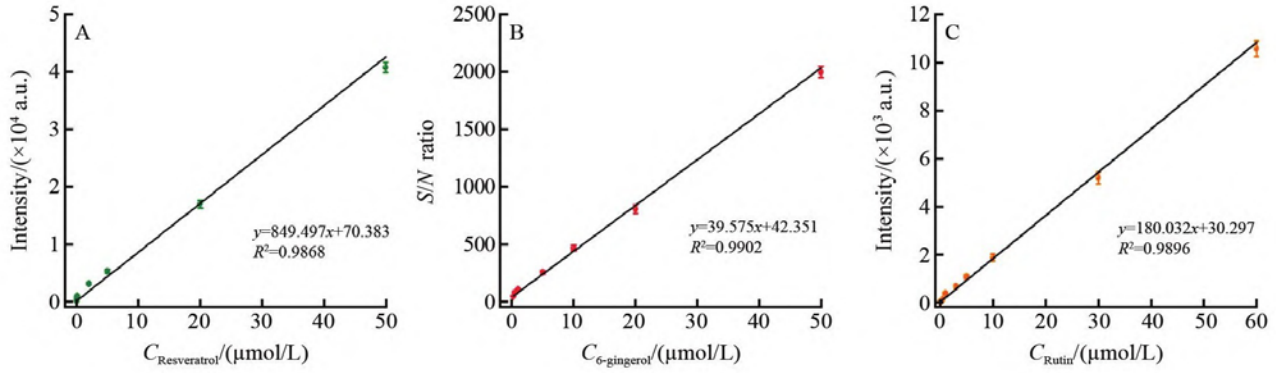

Figure 6. (A) Linear relationship between concentrations of resveratrol (0.01, 0.03, 0.06, 0.1, 2, 5, 20 and 50 μmol/L) and positive-ion MS peak intensity; (B) calibration curve between various concentrations of 6-gingerol (0.2, 0.5, 1, 5, 10, 20 and 50 μmol/L) and S/N ratio; (C) positive-ion MALDI MS analysis of rutin (0.05, 0.2, 0.5, 1, 3, 5, 10, 30, and 60 μmol/L) by Ni-2/Gr assisted MALDI MS.

Table 2. Corresponding *m/z*, ionization, linear range and limit of detection (LOD) of resveratrol, 6-gingerol and rutin with Ni-2/Gr as matrix

Target	Mass-to-charge ratio (*m/z*)	Ionization	Linear range (μmol/L)	Correlation coefficient (R^2)	LOD (μmol/L)
Resveratrol	229.025	$[M + H]^+$	0.01 ~ 50	0.9868	0.0038
	251.013	$[M + Na]^+$			
	267.064	$[M + K]^+$			
6-Gingerol	317.069	$[M + Na]^+$	0.2 ~ 50	0. 9902	0.09

chemiluminescence method[33] reported in the literature. The linear range of 6-gingerol analysis is better than the electrochemical method reported in the literature[34]. The MALDI MS method has a wide linear range[35] and low LOD value[36] in the analysis of rutin. Therefore, Ni-2/Gr as a new MALDI mass spectrometry matrix can be used for highly sensitive analysis of resveratrol, 6-gingerol and rutin.

3.3 Detection mechanism of Ni/Gr as MALDI matrix

In MALDI-TOF MS analysis, the matrix usually absorbs laser energy, and then transfers the energy to the analyte for the desorption and ionization of the substance to be measured. It is necessary to explain the ionization degree of the target by investigating the light absorption efficiency of MALDI matrix[37,38]. As shown in **Figure 7A**, observing the absorbance values of the synthesized Ni-1/Gr, Ni-2/Gr and Ni-5/Gr at 355 nm, it is found that Ni-2/Gr has the highest absorbance value and the lowest reflectivity value (**Figure 7B**). This shows that compared with Ni-1/Gr and Ni-5/Gr, Ni-2/Gr complex has the highest UV absorption capacity at 355 nm. At the same time, when using Ni-2/Gr complex as MALDI matrix, it can better absorb Nd: YAG 355 nm laser, transfer energy to the above drug small molecules (resveratrol, 6-gingerol and rutin), and promote the desorption and ionization of the small molecules to be tested. The above phenomena are consistent with MALDI MS experimental results (**Figures 4** and **5**). Therefore, Ni-2/Gr complex was selected as MALDI matrix to study the high-efficiency ionization analysis of small molecules.

In addition, the Ni/Gr composite shows a good S-type hysteresis loop[22] and has excellent strong magnetism (**Figures 7C** and **7D**). As shown in **Figure 7C**, the saturation magnetization values (MS) of Ni-1/Gr, Ni-2/Gr and Ni-5/Gr composites are 22.07, 31.36 and 48.22 emu/g, respectively. Because the content of Ni in Ni-5/Gr composite is the highest, the corresponding MS value is also the highest. As shown in **Figure 7D**, the coercivity (Hc) of Ni-1/Gr, Ni-2/Gr and Ni-5/Gr composites are 30.07, 35.84 and 21.43 Oe, respectively. Among them, Ni-2/Gr has the strongest Hc value, indicating that it has the strongest ability to resist external reverse magnetic field. Therefore, based on the high MS and Hc values of Ni-2/Gr, it can be used as a magnetic adsorbent[39] and MALDI matrix to enhance the mass spectrometry ionization efficiency of low concentration small molecules.

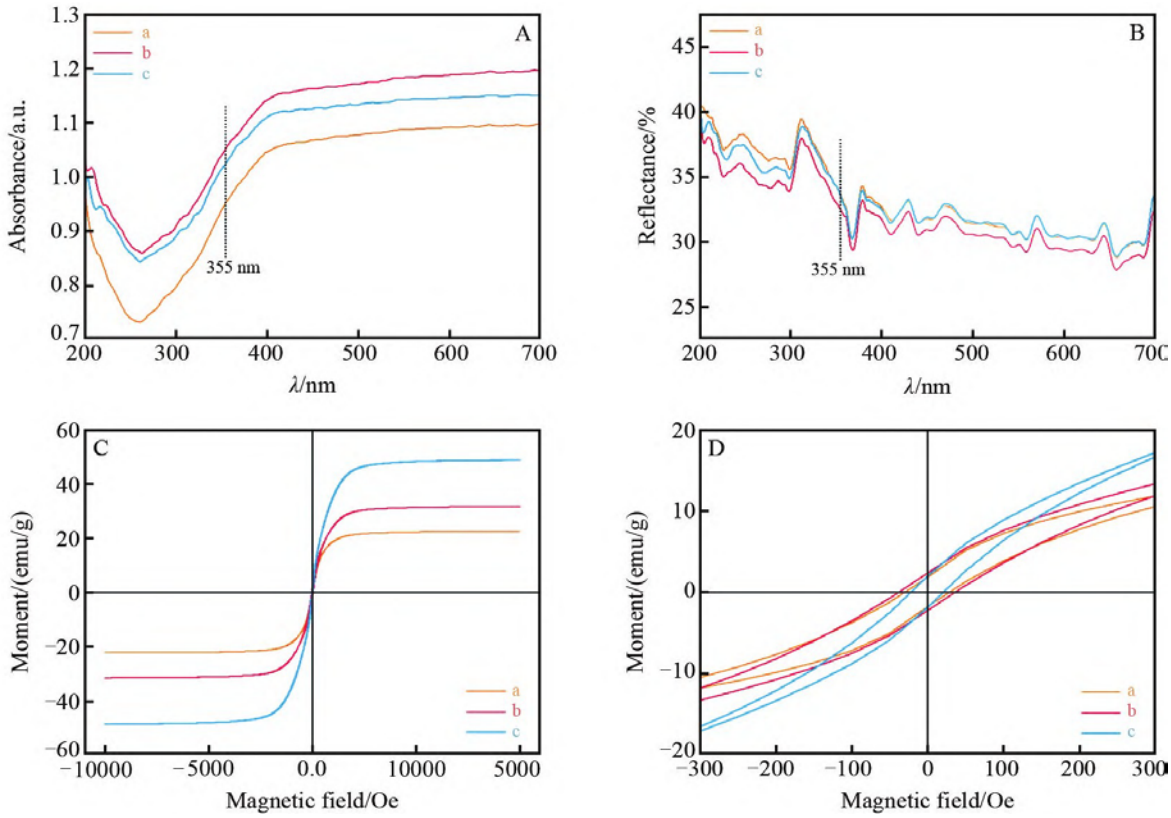

Figure 7. (**A**) UV-vis absorption spectra, (**B**) reflectance curves, (**C**) magnetic hysteresis loops and (**D**) enlarged curves of magnetic hysteresis loops between −300 and 300 Oe of (a) Ni-1/Gr, (b) Ni-2/Gr and (c) Ni-5/Gr in solid.

3.4 Enrichment of amino acid molecules based on Ni-2/Gr adsorbent

GR has a large specific surface area and contains a large number of sp^2 benzene ring structures. Therefore, a large number of molecules containing benzene rings can be captured through π–π action[40]. In order to improve the enrichment ability of Gr, magnetic nickel particles can be introduced to load on the surface of Gr, and the ability of Ni-2/Gr complex as adsorbent and MALDI matrix can be investigated. After the phenylalanine, tryptophan and tyrosine molecules were incubated with Ni-2/Gr solution for 20 minutes, the adsorbed amino acid molecules were separated magnetically under the action of an external magnetic field, and the solution and supernatant before and after enrichment were taken and dropped on the MALDI target plate for MS analysis. As shown in **Figure 8A**, before magnetic enrichment, the $[M + Na]^+$ peak of phenylalanine at *m/z* 188.029 can be observed, but it shows low ion peak intensity (curve a). After magnetic enrichment, high-intensity $[M + Na]^+$ peaks of phenylalanine appeared at *m/z* 188.029, and strong $[M + K]^+$ and $[M + 2Na-H]^+$ peaks of phenylalanine were observed at *m/z* 204.036 and 210.017 (curve b); in the supernatant after magnetic enrichment, only a very weak phenylalanine $[M + Na]^+$ peak (curve c) can be observed, indicating that Ni-2/Gr complex has good adsorption performance for phenylalanine. The magnetic enrichment of tryptophan and tyrosine molecules by Ni-2/Gr is shown in **Figure 8B** and **8C**. Similarly, after magnetic enrichment, tryptophan appears $[M + Na]^+$, $[M + K]^+$ and $[M + 2Na-H]^+$ peaks (curve b) at *m/z* 227.015, 243.061 and 249.078. Compared with supernatant before the enrichment (curve a) and after the enrichment (curve c), the tryptophan ion peak after magnetic enrichment presents high ionic strength and *S/N* value. Similarly, after magnetic enrichment, the peak intensity values of $[M + Na]^+$, $[M + K]^+$ and $[M + 2Na-H]^+$ of tyrosine molecules at *m/z* 204.028, 220.087 and 226.059 were significantly higher than those of the supernatant before and after enrichment. **Figure 8D** shows the optical photos before and after Ni-2/Gr magnetic enrichment of tyrosine. It can be seen that under the action of external magnetic field, Ni-2/Gr can be used for rapid enrichment of tyrosine molecules. In con-

clusion, Ni-2/Gr complex can be used not only as adsorbent, but also as MALDI matrix for the analysis of low concentration amino acids.

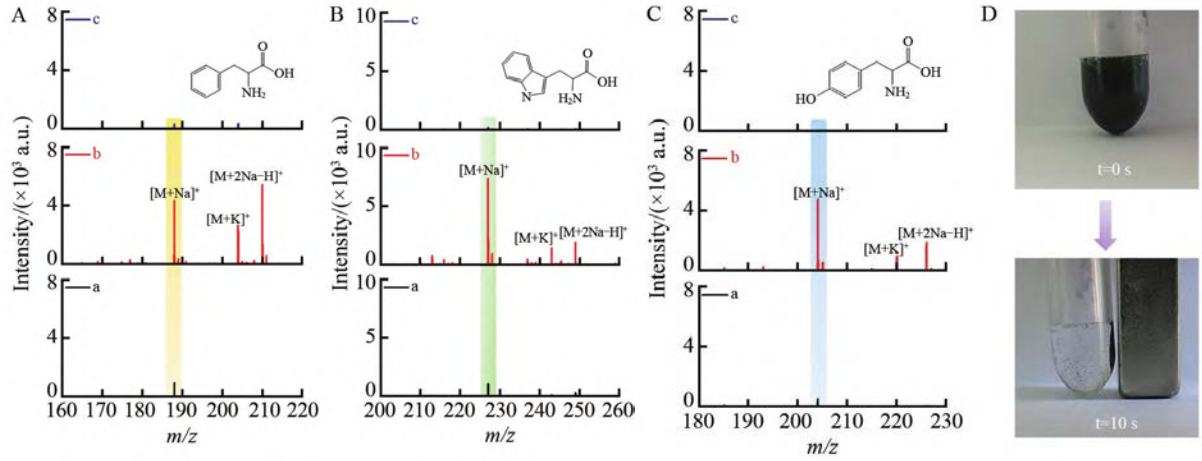

Figure 8. MALDI MS analyses of (**A**) L-phenylalanine, (**B**) L-tryptophan and (**C**) L-tyrosine with Ni-2/Gr as an adsorbent and matrix: (a) before enrichment; (b) after enrichment; (c) the corresponding supernatant. Concentrations of three amino acids are 50 μmol/L, respectively; (**D**) Optic images of L-tyrosine with Ni-2/Gr before and after enrichment.

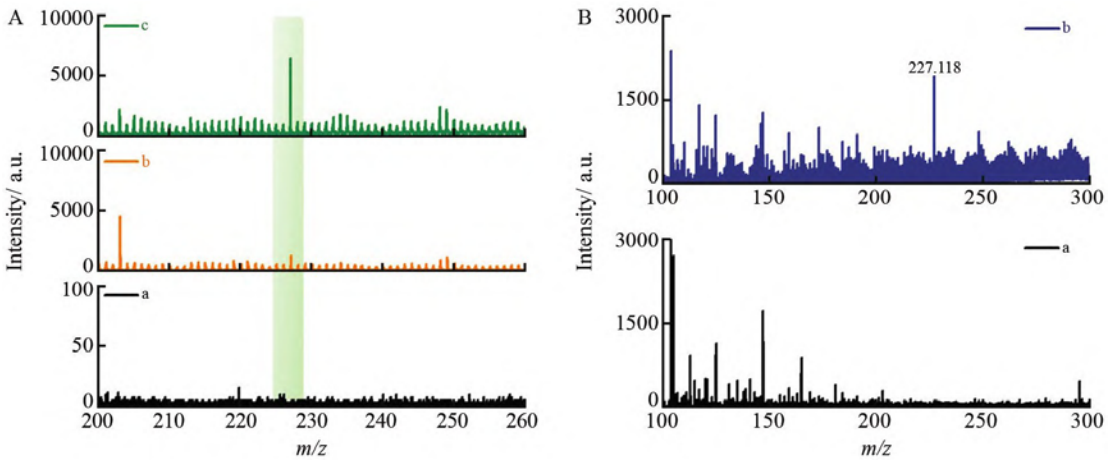

Figure 9. (**A**) MALDI MS analysis of (a) blank serum, L-tryptophan (50 μmol/L) spiked in mice serum bio-sample (b) before and (c) after enrichment with Ni-2/Gr as the adsorbent and matrix; (**B**) MS analysis of L-tryptophan (10 μmol/L) in mice serum bio-sample (a) before and (b) after enrichment.

3.5 Highly enriched mouse serum samples based on Ni-2/Gr matrix

In order to investigate the ability of this method to enrich amino acids in biological samples, the ion peaks of related molecules in blank mouse serum solution were investigated with Ni-2/Gr as matrix. It can be seen from curve a of **Figure 9A** that $[m + H]^+$, $[M + Na]^+$ and $[m + K]^+$ ion peaks of tryptophan were not observed in blank mouse serum solution. 50 μL of 10 mg/mL Ni-2/Gr matrix solution was added to 500 μL of mouse serum solution containing 50 μmol/L tryptophan, incubated with ultrasound for 20 min, and then magnetically separated under the action of an external magnet. 1 μL of the enriched solution was dropped onto a MALDI target plate, dried naturally, and then used for MALDI-TOF MS analysis.

Compared with that before magnetic enrichment (curve b), a stronger tryptophan $[M + Na]^+$ peak was observed at *m/z* 227.015 after enrichment (curve c). At the same time, compared with **Figure 8B**, after enrichment, although there are some other ion peak interference in the serum environment, it still has a high-intensity tryptophan $[M + Na]^+$ ion peak, indicating that it has strong anti-interference in the complex system. **Figure 9B** shows the mass spectra before and after adding 10 μmol/L tryptophan to mouse serum samples. Before magnetic enrichment (curve a), no ion peak of tryptophan was observed in serum samples of mice; after mag-

netic enrichment (curve b), the $[M + Na]^+$ peak of tryptophan was observed in mouse serum samples, indicating that Ni-2/Gr has the ability to adsorb and enrich low concentration tryptophan in the environment of mouse serum samples. Therefore, in the actual complex biological environment, Ni-2/Gr complex has good performance as enrichment material and MALDI matrix, which provides a new method for the screening of clinical biomarkers.

4. Conclusion

Ni-2/Gr composites were prepared by high temperature thermal reduction and characterized by various methods. Ni-2/Gr complex has the characteristics of high specific surface area, rich mesopores, a large number of sp^2 structures, strong UV absorption and high saturation magnetization value (MS). It can be used as a new MALDI matrix and adsorbent for highly sensitive detection of resveratrol, 6-gingerol, rutin drug molecules, efficient enrichment of phenylalanine, tryptophan, tyrosine, and analysis of low concentration tryptophan in actual serum samples. This method is expected to be used for highly sensitive screening and analysis of biological small molecules in clinical samples.

Acknowledgements

The project is supported by the National Natural Science Foundation of China (Nos. 22004082, 81771907) and the Science and Technology Innovation Project of Shanxi Provincial Department of Education (No. 2020L0173).

Conflict of interest

The authors declared no conflict of interest.

References

1. Tanaka K, Waki H, Ido Y, *et al*. Protein and polymer analyses up to m/z 100,000 by laser ionization time-of-flight mass spectrometry. Rapid Communications in Mass Spectrometry 1988; 2(8): 151–153.
2. Karas M, Hillenkamp F. Laser desorption ionization of proteins with molecular masses exceeding 10,000 daltons. Analytical Chemistry 1988; 60(20): 2299–2301.
3. Dallongeville S, Garnier N, Rolando C, *et al*. Proteins in art, archaeology, and paleontology: From detection to identification. Chemical Reviews 2016; 116(1): 2–79.
4. Kim M, Park JM, Yun TG, *et al*. TiO_2 nanowires from wet-corrosion synthesis for peptide sequencing using laser desorption/ionization time-of-flight mass spectrometry. ACS Applied Materials & Interfaces 2018; 10(40): 33790–33802.
5. Cornett DS, Reyzer ML, Chaurand P, *et al*. MALDI imaging mass spectrometry: Molecular snapshots of biochemical systems. Nature Methods 2007; 4(10): 828–833.
6. Wei J, Buriak JM, Siuzdak G. Desorption-ionization mass spectrometry on porous silicon. Nature 1999; 399(6733): 243–246.
7. Minhas RS, Rudd DA, Al Hmoud H Z, *et al*. Rapid detection of anabolic and narcotic doping agents in saliva and urine by means of nanostructured silicon SALDI mass spectrometry. ACS Applied Materials & Interfaces 2020; 12(28): 31195–31204.
8. Kawasaki H, Sugitani T, Watanabe T, *et al*. Layer-by-layer self-assembled mutilayer films of gold nanoparticles for surface-assisted laser desorption/ionization mass spectrometry. Analytical Chemistry 2008; 80(19): 7524–7533.
9. Silina YE, Meier F, Nebolsin VA, *et al*. Novel galvanic nanostructures of Ag and Pd for efficient laser desorption/ionization of low molecular weight compounds. Journal of The American Society for Mass Spectrometry 2014; 25(5): 841–851.
10. Su H, Li X, Huang L, *et al*. Plasmonic alloys reveal a distinct metabolic phenotype of early gastric cancer. Advanced Materials 2021; 33(17): 2007978.
11. Kim MJ, Park JM, Yun TG, *et al*. A TiO_2 nanowire photocatalyst for dual-ion production in laser desorption/ionization (LDI) mass spectrometry. Chemical Communications 2020; 56(32): 4420–4423.
12. Zhao Y, Xu Y, Gong C, *et al*. Analysis of small molecule compounds by matrix-assisted laser desorption ionization mass spectrometry with Fe_3O_4 nanoparticles as matrix. Chinese Journal of Analytical Chemistry 2021; 49(1): 103–112.
13. Shih YH, Chien CH, Singco B, *et al*. Metal-organic frameworks: New matrices for surface-assisted laser desorption-ionization mass spectrometry. Chemical Communications 2013; 49(43): 4929–4931.
14. Fan B, Zhou H, Wang Y, *et al*. Surface siloxane-modified silica materials combined with metal-organic frameworks as novel MALDI matrixes for the detection of low-MW compounds. ACS Applied Materials & Interfaces 2020; 12(33): 37793–37803.
15. Dong X, Cheng J, Li J, *et al*. Graphene as a novel matrix for the analysis of small molecules by MALDI-TOF MS. Analytical Chemistry 2010; 82(14): 6208–6214.
16. Shi R, Dai X, Li W, *et al*. Hydroxyl-group-dominated graphite dots reshape laser desorption/ionization mass spectrometry for small biomolecular analysis and imaging. ACS Nano 2017; 11(9): 9500–9513.

17. Xu S, Li Y, Zou H, *et al*. Carbon nanotubes as assisted matrix for laser desorption/ionization time-of-flight mass spectrometry. Analytical Chemistry 2003; 75(22): 6191–6195.
18. Chen S, Zheng H, Wang J, *et al*. Carbon nanodots as a matrix for the analysis of low-molecular-weight molecules in both positive-and negative-ion matrix-assisted laser desorption/ionization time-of-flight mass spectrometry and quantification of glucose and uric acid in real samples. Analytical Chemistry 2013; 85(14): 6646–6652.
19. Luo P, Wang L, Jiang L, *et al*. Application of graphdiyne in surface-assisted laser desorption ionization mass spectrometry. ACS Applied Materials & Interfaces 2020; 13(1): 1914–1920.
20. Zhao H, Li Y, Wang J, *et al*. Dual-ion-mode MALDI MS detection of small molecules with the O-P, N-doped carbon/graphene matrix. ACS Applied Materials & Interfaces 2018; 10(43): 37732–37742.
21. Lu L, Zheng G, Wang M, *et al*. Microwave-prepared mesoporous graphene as adsorbent and matrix of surface-assisted laser desorption/ionization mass spectrometry for the enrichment and rapid detection of polyphenols in biological samples. Talanta 2021; 222: 121365.
22. Sheng A, Yang Y, Yan D X, *et al*. Self-assembled reduced graphene oxide/nickel nanofibers with hierarchical core-shell structure for enhanced electromagnetic wave absorption. Carbon 2020; 167: 530–540.
23. Li S, Liu J, Sun J, *et al*. Co-NC as adsorbent and matrix providing the ability of MALDI MS to analyze volatile compounds. Chinese Chemical Letters 2021; 32(1): 62–65.
24. Baruah A, Mondal S, Sahoo L, *et al*. Ni-Fe-layered double hydroxide/N-doped graphene oxide nanocomposite for the highly efficient removal of Pb (II) and Cd (II) ions from water. Journal of Solid State Chemistry 2019; 280: 164–170.
25. Li N, Li S, Li T, *et al*. Co-incorporated mesoporous carbon material-assisted laser desorption/ionization ion source as an online interface of in vivo microdialysis coupled with mass spectrometry. Analytical Chemistry 2020; 92(7): 5482–5491.
26. Wang J, Manga KK, Bao Q, *et al*. High-yield synthesis of few-layer graphene flakes through electrochemical expansion of graphite in propylene carbonate electrolyte. Journal of the American Chemical Society 2011; 133(23): 8888–8891.
27. Wang C, Zhao H, Wang J, *et al*. Atomic Fe hetero-layered coordination between g-C_3N_4 and graphene nanomeshes enhances the ORR electrocatalytic performance of zinc-air batteries. Journal of Materials Chemistry A 2019; 7(4): 1451–1458.
28. Fu G, Yan X, Chen Y, *et al*. Boosting bifunctional oxygen electrocatalysis with 3D graphene aerogel-supported Ni/MnO particles. Advanced Materials 2018; 30(5): 1704609.
29. Xu W, Wang GS, Yin PG. Designed fabrication of reduced graphene oxides/Ni hybrids for effective electromagnetic absorption and shielding. Carbon 2018; 139: 759–767.
30. Balamurugan J, Nguyen TT, Kim NH, *et al*. Novel core-shell CuMo-oxynitride@ N-doped graphene nanohybrid as multifunctional catalysts for rechargeable zinc-air batteries and water splitting. Nano Energy 2021; 85: 105987.
31. Yang X, Guo Q, Yang J, *et al*. Synergistic effects of layer-by-layer films for highly selective and sensitive electrochemical detection of trans-resveratrol. Food Chemistry 2021; 338: 127851.
32. Zhang C, Ping J, Ye Z, *et al*. Two-dimensional nanocomposite-based electrochemical sensor for rapid determination of trans-resveratrol. Science of the Total Environment 2020; 742: 140351.
33. Wang L, Zhang Z. Molecular imprinted polymer-based chemiluminescence imaging sensor for the detection of trans-resveratrol. Analytica Chimica Acta 2007; 592(2): 115–120.
34. Chaisiwamongkhol K, Ngamchuea K, Batchelor-McAuley C, *et al*. Electrochemical detection and quantification of gingerol species in ginger (Zingiber officinale) using multiwalled carbon nanotube modified electrodes. Analyst 2016; 141(22): 6321–6328.
35. Cheng C, Huang Y, Wang J, *et al*. Anodic electrogenerated chemiluminescence behavior of graphite-like carbon nitride and its sensing for rutin. Analytical Chemistry 2013; 85(5): 2601·2605.
36. Zhan T, Sun X, Wang X, *et al*. Application of ionic liquid modified carbon ceramic electrode for the sensitive voltammetric detection of rutin. Talanta 2010; 82(5): 1853–1857.
37. Yang J, Zhang W, Zhang H, *et al*. Polydopamine-modified sub strates for high-sensitivity laser desorption ionization mass spectrometry imaging. ACS Applied Materials & Interfaces 2019; 11(49): 46140–46148.
38. Kim S, Kwon S, Kim Y. Nanomaterials 2021; 11(2): 288–306.
39. Kawasaki H, Nakai K, Arakawa R, *et al*. Functionalized graphene-coated cobalt nanoparticles for highly efficient surface-assisted laser desorption/ionization mass spectrometry analysis. Analytical Chemistry 2012; 84(21): 9268–9275.
40. Shi C, Meng J, Deng C. Enrichment and detection of small molecules using magnetic graphene as an adsorbent and a novel matrix of MALDI-TOF-MS. Chemical Communications 2012; 48(18): 2418–2420.